Front. Environ. Sci. Eng. 2020, 14(4): 71
https://doi.org/10.1007/s11783-020-1250-0

RESEARCH ARTICLE

A study of peroxyacetyl nitrate at a rural site in Beijing based on continuous observations from 2015 to 2019 and the WRF-Chem model

Yulu Qiu[1,2,3], Zhiqiang Ma (✉)[1,2,3], Weili Lin[4], Weijun Quan[2,3], Weiwei Pu[2,3], Yingruo Li[2,3], Liyan Zhou[2,3], Qingfeng Shi[2,3]

1 Institute of Urban Meteorology, China Meteorological Administration, Beijing 100089, China
2 Beijing Shangdianzi Regional Atmosphere Watch Station, Beijing 101507, China
3 Environmental Meteorology Forecast Center of Beijing-Tianjin-Hebei, Beijing 100089, China
4 College of Life & Environmental Science, Minzu University of China, Beijing 100081, China

HIGHLIGHTS

- PAN concentrations at a rural site near Beijing were monitored from 2015 to 2019.
- PAN concentrations exhibited high values in spring and low values in winter.
- Anomalously southerlies induced extreme high PAN concentration in spring 2018.

GRAPHIC ABSTRACT

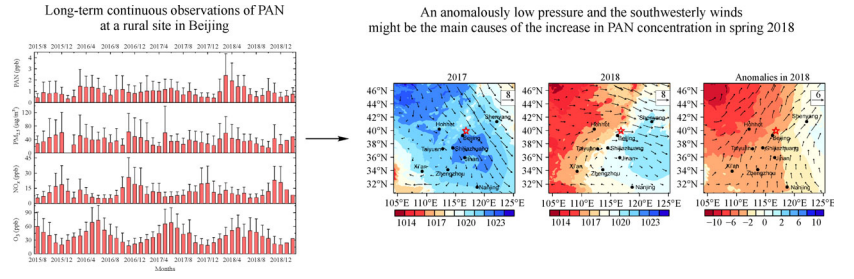

ARTICLE INFO

Article history:
Received 22 December 2019
Revised 26 February 2020
Accepted 20 March 2020
Available online 28 April 2020

Keywords:
PAN
Ozone
Beijing
WRF-Chem

ABSTRACT

Peroxyacetyl nitrate (PAN) is one of the most important photochemical pollutants and has aroused much concern in China in recent decades. However, few studies described the long-term variations in PAN in China. In this study, we continuously monitored the PAN, O_3 and NO_x concentrations at a regional background site near Beijing from August 2015 to February 2019. Based on the observed concentrations and climate data, we analyzed the seasonal PAN variations. The results revealed that the monthly mean PAN concentration ranged from 0.33–2.41 ppb, with an average value of 0.94 ppb. The PAN concentration exhibited a distinct seasonal variation, with high values in spring and low values in winter. After analyzing the corresponding meteorological data, we found that stronger ultraviolet (UV) radiation, a relatively longer lifetime and a higher background PAN concentration contributed to the high PAN concentrations in spring. In addition, with the utilization of the WRF-Chem (Weather Research and Forecasting with Chemistry) model, the cause of the extremely high PAN concentration in spring 2018 was determined. The model results demonstrated that an anomalously low pressure and the southwesterly winds in northern China might be the main causes of the increased PAN concentration in Beijing and its surrounding area in spring 2018.

1 Introduction

Peroxyacetyl nitrate (PAN, $CH_3COO_2NO_2$) is generally regarded as a key component of photochemical smog formed through reactions among volatile organic compounds (VOCs) and NO_x (Singh and Salas, 1989; Fischer et al., 2014). The main PAN removal processes include thermal decomposition and ultraviolet (UV) photolysis (Talukdar et al., 1995; Seinfeld and Pandis, 2006). Because of its dependence on temperature, PAN is quite stable and serves as a reservoir for NO_x in the middle and upper troposphere or at low temperatures (Singh and Hanst, 1981; Singh et al., 1986; Fischer et al., 2010). High PAN concentrations cause plant damage (Taylor, 1969; Temple

✉ Corresponding author
E-mail: zqma@ium.cn

and Taylor, 1983) and eye irritation (Heuss and Glasson, 1968), arousing much concern worldwide in recent years.

A number of observational studies on PAN have been conducted in North America, Europe, and Asia in recent decades, indicating that the PAN concentrations range from the pptv level at background sites (Beine et al., 1996; Zhang et al., 2009; Fischer et al., 2010) or in the middle and upper troposphere (Singh et al., 1985; Schmitt and Volz-Thomas, 1997) to the ppbv level at urban sites (Tanner et al., 1988; Rappenglück et al, 1993; Sun and Huang, 1995; Lee et al., 2013). More recently, numerous observational studies on PAN have been conducted in China, and the basic features, regional transport and sources of PAN have been investigated (Zhang et al., 2009; Liu et al., 2010; Wang et al., 2010; Gao et al., 2014; Xue et al., 2014; Zhang et al., 2014; Zhang et al., 2015; Liu et al., 2018; Zhu et al., 2018; Qiu et al., 2019a; 2019b). Most of these studies recognized that the PAN concentration peaked in the afternoon and then decreased, which could be attributed to the active photochemical reactions due to intensive solar radiation and strong thermal decomposition in the daytime. In addition, some of these studies investigated the impact of regional transport on local PAN concentrations. For example, by comparing the measured PAN concentrations at a suburban site in Lanzhou and at a remote site on Mt. Waliguan during summer in 2006, Zhang et al. (2009) found that the average PAN concentrations were 0.76±0.89 ppbv and 0.44±0.16 ppbv, respectively, and proved that the PAN pollution events at the Mt. Waliguan site were mostly associated with the transport of air masses from Lanzhou, a megacity 260 km to the east of Mt. Waliguan. By combining observational data and model results, Qiu et al. (2019a) investigated the PAN features during a pollution event in winter in Beijing and reported that local sources accounted for approximately 15%–30% of the mean PAN concentration over most of Beijing, lower than the proportion attributed to $PM_{2.5}$ (25%–60%). PAN is formed through reactions among VOCs and NO_x. Studies have also determined the contributions of individual VOC species. Using the explicit photochemical model, Xue et al. (2014) quantified the contributions of individual precursors to PAN in Beijing in the summer of 2008 and reported that the predominant VOC precursors at the suburban and downtown sites were biogenic isoprene and anthropogenic reactive aromatics, respectively.

Most of the above studies concentrated on PAN characteristics during a pollution event or in a specific season. Thus far, long-term continuous studies on PAN are still rare in China. However, numerous studies concerning long-term PAN observations have been conducted in other countries or regions worldwide (Brice et al., 1984; Gaffney et al., 1993; Penkett and Brice, 1986; Beine and Krognes, 2000; McFadyen and Cape, 2005; Lee et al., 2013). These researchers recognized that seasonally averaged maximum PAN concentrations occurred in spring with values lower than 1 ppb, both for clean background sites (Penkett and Brice, 1986; Moxim et al., 1996; Beine and Krognes, 2000; McFadyen and Cape, 2005; Pandey Deolal et al., 2014) and polluted urban areas (Lee et al., 2013). However, it was debated whether the PAN concentration was higher in summer or winter. Studies suggested that the summertime PAN concentrations were higher than those in winter due to the strong photochemical reactions in summer (Rappenglück et al, 1993; McFadyen and Cape, 2005). Other studies, however, held the opposite view in that the wintertime PAN concentrations were higher than those in summer (Brice et al., 1984; Penkett and Brice, 1986; Gaffney et al., 1993; Beine and Krognes, 2000; Lee et al., 2013) as a result of atmospheric circulation changes.

Beijing, the political and cultural center of China, is located in the north of the North China Plain (NCP) and is surrounded by mountains on three sides. In recent decades, the population of Beijing has remained at a high level in association with active urbanization and economic development. Moreover, accompanying air pollution has occurred (Wang et al., 2014; Yin et al., 2019). A few studies have investigated the characteristics of PAN in this region (Zhang et al., 2014; Qiu et al., 2019a; 2019b). However, these studies focused on its features during pollution events or in a single season. Continuous long-term observational studies on PAN are comparatively rare in the NCP, and the seasonal PAN variations are still unclear in this region. In addition, long-term observation could facilitate investigation of the interannual variation in PAN concentration in this region, and through modeling, the observations could also help determine the cause of the extremely high PAN concentrations in certain seasons.

Considering the lack of long-term continuous PAN observations in the NCP, we will examine the seasonal and interannual PAN variations at a remote site near Beijing from 2015 to 2019, and cause of seasonal variation will also be analyzed. This study is the first to present 3-year continuous measurement results for PAN in China and to investigate the cause of its seasonal variation. In addition, we investigate the extremely high PAN concentrations in certain seasons, and the causes of these variations are examined using a chemical numerical model. This study could help us further understand the photochemical level in the polluted NCP region, and help authorities to implement control strategies.

2 Experiment

2.1 Field experiments

Figure 1 shows the detailed geophysical location of the Shangdianzi site (SDZ, 40°39′N, 117°07′E, 293.9 m a.s.l.), as well as the anthropogenic NO_x emission rates. The SDZ

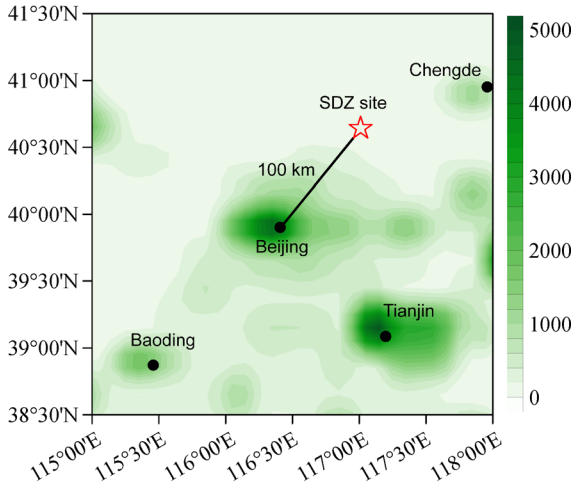

Fig. 1 The anthropogenic emission rates of NO_x (unit: $1.0e^{-12}$ $kg/m^2/s$) in 2010 and the location of the SDZ sampling site (red star). The emission rates are derived from the MIX emission inventory in 2010 (Li et al., 2017).

site is one of the regional Global Atmosphere Watch (GAW) stations in China, and is located in the northern part of the NCP, approximately 100 km north-east of the urban center. The rural site is surrounded by extensive vegetation and sparsely populated small villages and has fewer anthropogenic sources. Therefore, it is usually regarded as a regional background site in the NCP region.

The ambient PAN concentration was measured with an online gas chromatograph equipped with an electron capture detector (GC-ECD) at a time resolution of 5 min. The limit of detection was 50 ppt. The capillary column was mounted in a compact temperature-controlled oven which maintained the temperature at 12°C. The temperature of ECD was set at 50°C with fluctuations of ±0.2°C. To calibrate the GC-ECD instrument, PAN was synthesized via the 285-nm photolysis of acetone in the presence of a calibrated NO flow with a reaction yield of 93% PAN. The NO standard gas (Linde SPECTRA Environmental Gases) was prepared at 0.97 ppm. A regular calibration check was conducted every month to guarantee the quality of the PAN results. The PAN measurement campaigns at the rural site were conducted from August 2015 to February 2019.

The O_3, $PM_{2.5}$, and NO_2 concentrations were also measured simultaneously at the SDZ site using a UV photometric O_3 analyzer (model 49i, Thermo Electron Corporation, USA), a TEOM-1405 analyzer, and a laser-based (cavity-enhanced laser absorption spectroscopy) nitrogen dioxide analyzer (Los Gatos Research, Inc., USA), respectively. As O_3 is the most important photochemical pollutant, the relationship between O_3 and PAN can help us better understand the photochemical pollution level in this region. NO_2 is the main PAN precursor. In addition, meteorological parameters, such as temperature, relative humidity, precipitation, wind speed and direction, and UV-A and UV-B radiation levels were also recorded at the SDZ site.

2.2 Model simulations

In this study, we also sought to obtain the seasonal variations in PAN in northern China and determine the cause of interannual variations. We found that the PAN concentration in the spring of 2018 reached extremely high values when compared with the PAN concentration in other seasons (shown in Section 3). However, as the Chinese government has realized the urgency of reducing the atmospheric $PM_{2.5}$ concentration since 2013, it has adopted a series of measures to reduce the precursors of $PM_{2.5}$, such as SO_2 and NO_x, and the anthropogenic emission rate of NO_x did indeed decrease by approximately 23% over northern China from 2013 to 2017 (Li et al., 2019). Although the importance of VOC reduction to air quality has been emphasized since 2018, VOCs slightly increased from 2013 to 2017 over northern China (Li et al., 2019). These changes in VOC emissions are unlikely to be the cause of the extremely high PAN concentration in spring 2018. Thus, we conducted model simulations at fixed anthropogenic emission rates in the spring seasons of 2017 and 2018 to determine the impact of climatic and meteorological factors on the interannual PAN variations in northern China.

The WRF-Chem model version 3.9.1.1 was utilized in our study. The model domain has a horizontal resolution of 9 km, covering northern China, which follows the domain configuration in Qiu et al. (2019b). The parameterization methods used in this study consist of the CBM-Z gas-phase scheme (Zaveri and Peters, 1999), the Model for Simulating Aerosol Interactions and Chemistry (MOSAIC) (Zaveri et al., 2008) with four sizes of bins, the WSM 6-class microphysics scheme (Hong and Jade Lim, 2006), the Goddard shortwave radiation scheme (Chou et al., 1998), the RRTM longwave radiation scheme (Mlawer et al., 1997), and the Yonsei University boundary layer scheme (Hong et al., 2006). The Multi-resolution Emission Inventory for China (MEIC) for 2016 (www.meicmodel.org) developed by Tsinghua University was used here for the anthropogenic emission data. Biogenic emissions were calculated online from the Model of Emissions of Gases and Aerosols from Nature (MEGAN) (Guenther et al., 2006). We conducted simulations in March of 2017 and 2018 using the same anthropogenic emissions but different meteorological fields. Thus, the difference between the two simulations could be attributed to the impact of meteorological changes. In addition, the integrated process analysis method was also used in this study to determine the most significant process affecting the seasonal PAN variations in northern China, which could have great impacts on our understanding of high-PAN events.

3 Results

3.1 Data overview

Figure 2 shows the observed monthly concentrations of PAN, $PM_{2.5}$, O_3 and NO_x at the SDZ site from August 2015 to February 2019. The monthly mean PAN concentrations varied from 0.33–2.41 ppb at the SDZ site, with an average value of 0.94 ppb. The maximum and minimum mean PAN concentrations occurred in March 2018 and January 2016, respectively. In general, the PAN concentration showed a notably high level in spring, especially in the spring of 2018, and the maximum monthly mean value exceeded 2 ppb. Relatively lower PAN concentrations were usually observed in winter. Recently, some studies using long-term O_3 observation data in the NCP reported that the O_3 concentration in this area has experienced increases in recent years before 2017 (Ma et al., 2016; Li et al., 2019). As the second most important photochemical species, the long-term PAN trend in China is still unclear due to a lack of measurements. The observed PAN concentration data for a period longer than 3 years were analyzed in our study, and after 2015, the maximum PAN concentrations at the SDZ site occurred in 2018. Although we could not conclude that the PAN concentration showed an increasing trend in recent years based only on the 3-year data, this study should still draw attention to the photochemical levels in Beijing and its surrounding areas as well as the impacts of these pollutants on human health and plants in recent years.

Figure 2 also shows the monthly variations in O_3 and NO_x. The photochemical pollutant O_3 usually reached maximum concentrations from May to August annually at the background site, which occurred slightly later than those of PAN. Similarly, the minimum O_3 concentration was observed in winter due to the weak solar radiation and low temperature. As a precursor of PAN and O_3, the NO_x concentration exhibited the opposite seasonal variation and exhibited higher values during the heating period (autumn and winter) over northern China.

Figure 3 displays the diurnal cycles of PAN averaged over 2015–2019 in each season at the SDZ site. In general, PAN exhibited distinct diurnal patterns and reached the maximum mean value from 16:00–18:00 (local time) at the background site. This peak occurred slightly later than in previous results at urban sites (Liu et al., 2010; Zhang et al., 2017), where peak values were observed from 14:00–15:00 (local time). As the SDZ site is located in the north-east of an urban area, it might be highly affected by the southerlies with relatively high PAN concentrations in the afternoon, whereby the peak time at the SDZ site could be delayed. In winter, the PAN concentration reached its maximum value slightly earlier than in the other seasons, and the diurnal variation was much weaker than those in the other seasons. These differences could be attributed to the low production and long lifetime of PAN during the

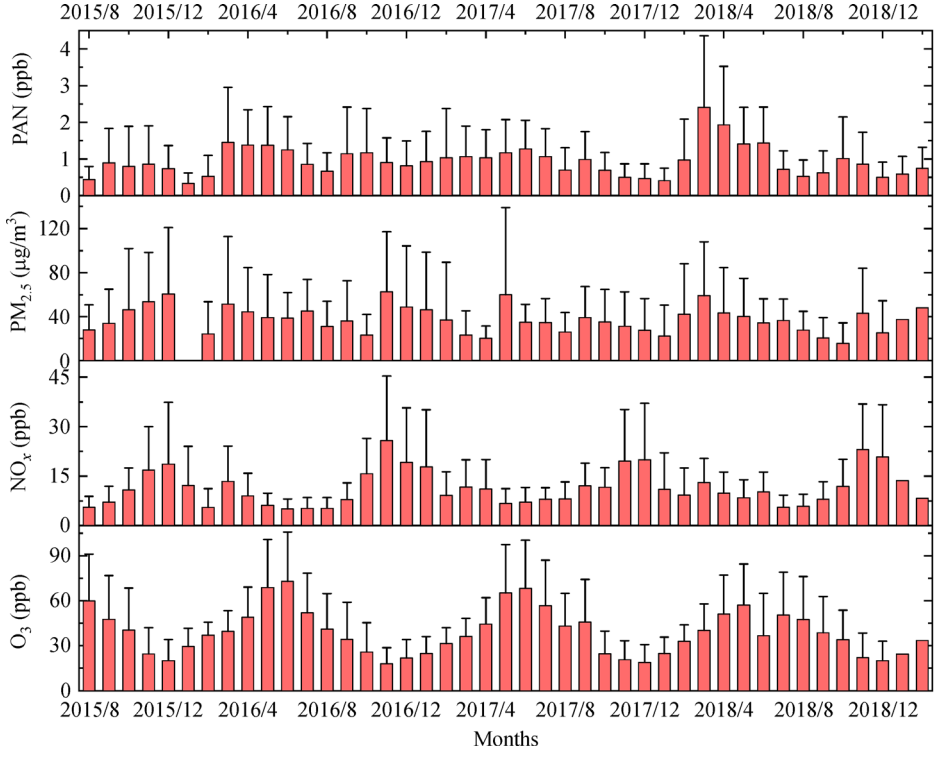

Fig. 2 Observed monthly concentrations of PAN (ppb), $PM_{2.5}$ ($\mu g/m^3$), O_3 (ppb) and NO_x (ppb) at the SDZ site from August 2015 to February 2019. The whiskers represent the standard deviation in each month.

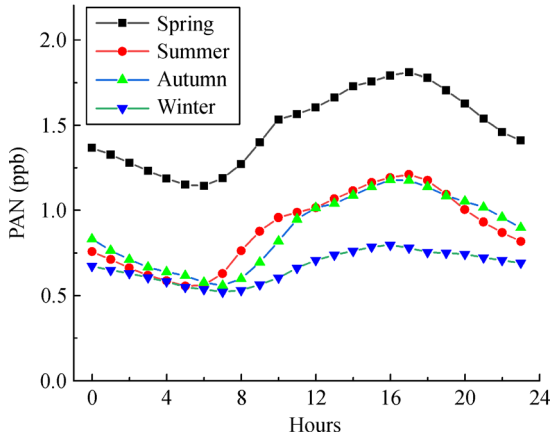

Fig. 3 Observed diurnal variations in the PAN concentration at the SDZ site in each season averaged from August 2015 to February 2019.

winter. In winter, the weak solar radiation could lead to weak photochemical reaction; thus, the production of PAN during the daytime was low. Furthermore, the PAN lifetime extended due to the lower temperature in winter, which facilitated the accumulation of PAN during the nighttime.

3.2 Causes of the high PAN concentrations in spring

As shown in Section 3.1, the maximum seasonal mean concentrations occurred in spring, which were 51.0% higher than the values averaged over the whole observation period. Additionally, previous studies suggested that the PAN concentrations in spring were 16%–31% higher than the annual mean values at both background sites and urban areas (Beine and Krognes, 2000; Lee et al., 2013). The PAN concentration is determined by meteorology, precursor emission rates, and background concentration. Next, we will discuss the cause of the high PAN concentrations at the SDZ site from these three aspects.

In terms of emissions, previous studies suggested that the NO_x emission rates in China reach higher values in late autumn and winter (Li et al., 2017), mainly due to the higher energy demand for residential heating. However, for the formation of PAN, NO_x is more abundant in the atmosphere at a level of tens of ppb at the SDZ site, while VOC species are at the ppt to ppb levels. Therefore, the PAN concentration is largely determined by the variation in VOC emissions across this region. As the SDZ site is a background site, one of the most important VOC PAN precursors at the SDZ site is biogenic isoprene. Monson et al. (1992) proved that isoprene emission rates increased with the temperature when the leaf temperature was lower than 40°C, thus explaining the high isoprene concentration in summer. Li et al. (2013) also reported that the concentration of isoprene in July was highest and that in January was lowest in Beijing, with monthly mean concentrations of 0.1–1.8 ppb. Therefore, we can conclude that the emission of precursors promotes PAN formation in summer compared to the other seasons, which could not explain the high concentration in spring at the SDZ site.

The formation and decomposition of PAN are highly affected by meteorological parameters, such as radiation, temperature and atmospheric dispersion ability. PAN is formed through the reaction between the $CH_3C(O)O_2$ (PA) radical and NO_2, and radiation is vital for the formation of the PA radical. Figure 4 shows the observed time series of ultraviolet-A (UV-A) and ultraviolet-B (UV-B) radiation at the SDZ site during the observation period. We see clear seasonal changes in UV radiation, which reached maximum values from spring to summer. Statistical results showed that the seasonal UV-A (UV-B) radiation levels in spring and summer were 20.9 (0.32) and 21.9 (0.35) W/m^2, respectively, which are 21.9% (26.1%) and 27.3% (36.1%), respectively, higher than the average values over the whole period. This discrepancy could explain the relatively higher PAN concentrations during spring and summer. However, Fig. 4 also shows that the UV radiation level in the summer of 2018 was relatively lower than that in the other years due to the strong precipitation in July and August 2018. The corresponding PAN concentrations in July and August 2018 were also relatively lower. Therefore, we conclude that the relatively intense radiation could

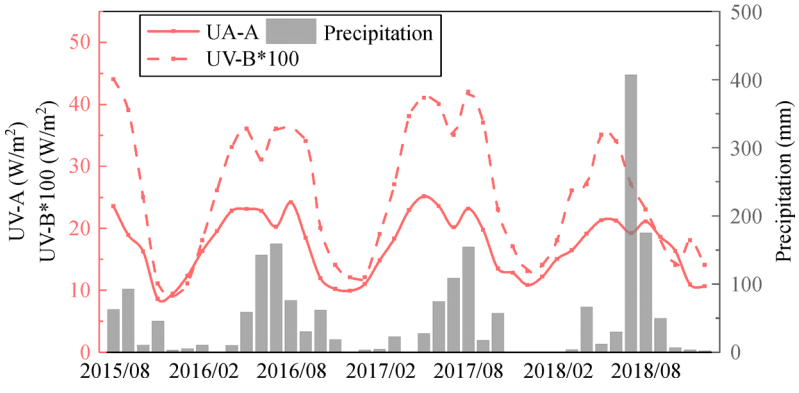

Fig. 4 Observed monthly variations in ultraviolet-A (UV-A) (W/m^2), ultraviolet-B (UV-B) radiation (W/m^2) and precipitation (mm) at the SDZ site from August 2015 to December 2018.

contribute to the active photochemical reactions in spring and summer.

Another impact factor of the PAN concentration in the atmosphere is its lifetime. Figure 5 shows the seasonal variations in the PAN family (PAN and PA radicals) lifetime at the SDZ site, which follows the calculation method of Qiu et al. (2019b). The mean temperature values were 8.9°C, 24.1°C, 9.9°C and –4.6°C in spring, summer, fall and winter, respectively, and the corresponding median lifetimes of the PAN family were 49.5 h, 7.3 h, 119.7 h and 1020.6 h. Thus, the lifetime of PAN and PA radicals could reach several to tens of days most of the time, except in summer, when thermal PAN decomposition was more intensive due to the higher temperature. This effect might largely explain the relatively lower PAN concentration in summer than in spring, despite the high photochemical activity in summer.

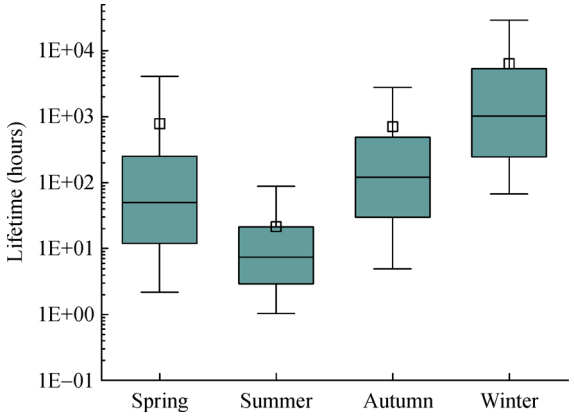

Fig. 5 Box plots of the PAN family lifetime at the SDZ site averaged from August 2015 to February 2019.

The background level is also a substantial component of the PAN concentration. As stated previously, seasonally averaged maximum PAN concentrations were reported in spring at clean background sites around the world (Penkett and Brice, 1986; Moxim et al., 1996; Beine and Krognes, 2000; McFadyen and Cape, 2005; Pandey Deolal et al., 2014). These results could be indicative of a certain background average in those regions and surrounding areas and confirmed that the global background PAN concentration in the Northern Hemisphere was high in spring, which might also contribute to the measured high PAN concentration at the SDZ site. In addition, we calculated the background PAN concentration at the SDZ site following the method of Bukowiecki et al. (2002), who utilized small percentiles over a certain time period to represent the background NO_2 concentration. Here, we chose 5% as the percentile limit following the method in Bukowiecki et al. (2002) and 7 days as the moving interval because the duration of a pollution event is usually shorter than one week. Figure 6 shows the calculated hourly (a) and monthly (b) PAN background concentrations at the SDZ site. Figure 6(b) shows that the monthly averaged background PAN concentrations were in the range of 0.1–0.8 ppb. Statistical results further revealed that the mean background concentration in spring was 0.42 ppb, which was 55.5% higher than the average concentration over the whole observation period. Indeed, there existed uncertainties in calculating the exact background concentration, but we could qualitatively determine in this study that the increase in PAN background concentration contributed to the measured PAN concentration at the SDZ site to a certain extent.

From the above analysis, we conclude that the relatively intense radiation, long lifetime and high background

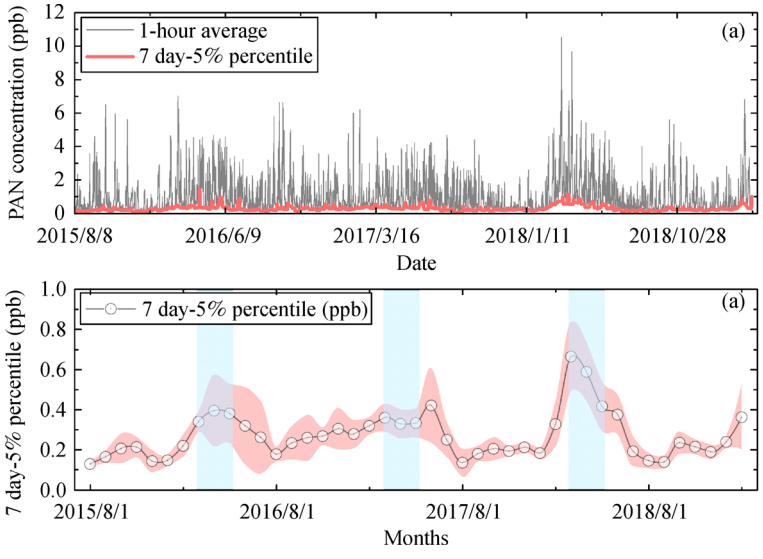

Fig. 6 (a) Hourly observed PAN concentrations (ppb, black line) and 5% percentile (ppb, red line) over 7 days during the observation period at the SDZ site. (b) Monthly averaged values of the 7 day-5% percentile concentrations (ppb, black line with circle) and the corresponding standard deviation (red contour). The blue shaded areas denote the springtime.

concentration contributed to the peak PAN concentrations in the springtime at the SDZ site. Although a high photochemical activity and high isoprene emissions occurred in the summertime, the decrease in PAN due to thermal and wet deposition might suppress the concentration increase.

3.3 Exploration of the extremely high PAN concentrations in March 2018

As discussed in Section 3.2, the PAN concentration at the SDZ site exhibited notable seasonal variations, usually with maximum values in spring. Moreover, the PAN concentrations in spring showed interannual variations. As shown in Fig. 2, the monthly maximum PAN concentration at the SDZ site in March 2018 was 2.4 ppb. Figure 7 compares the mean PAN concentrations in March from 2016 to 2018. The PAN concentration in March of 2018 was the highest among the three years and was 47.0% higher than the mean value averaged from March 2016 to 2018. The O_3, NO_x and $PM_{2.5}$ concentrations were all the highest in 2018 and the lowest in 2017, but the change rates differed. For example, the $PM_{2.5}$ concentration in March 2018 was 32.6% higher than the mean value from 2016 to 2018, while the O_3 and NO_x ratios were only 4.1% and 2.6%, respectively. Figure 7 shows that the PAN and $PM_{2.5}$ change rates were of the same magnitude and were much higher than those of O_3 and NO_x.

As noted in Section 2, the anthropogenic NO_x emission rates decreased in recent years over northern China, whereas the VOCs emission rates changed very little. Thus, the increase in PAN concentration in March 2018 could very likely be attributed to variation in meteorological conditions. To examine the impact of variation in meteorological factors on the observed high PAN concentration in March 2018, we conducted two simulations with the same anthropogenic emission rates but with different meteorological fields (March 2017 vs. March 2018). Here, we chose March to represent the whole spring season to minimize the computing cost. Figure 8 shows the simulated differences between the PAN concentrations in March of 2018 and 2017. The PAN concentrations in March 2018 were notably higher than those in 2017 over most of the NCP region. The increase rates ranged from 40%–60% in Beijing and the northern part of the NCP region. In the daytime, the change rates in the northern part of Beijing even exceeded 60%.

To diagnose the contributions of each physical or chemical process to the variations in PAN concentration, we utilized the integrated process rate analysis method in the WRF-Chem model, which has been recently used in studying the contribution of processes to pollutant concentrations in China (Jiang et al., 2012; Gao et al., 2018; Qiu et al., 2019b; Chen et al., 2019). Figure 9 shows the simulated changes in PAN concentration by vertical mixing, chemical reactions, and advection in these two months over the NCP region during the daytime as well as the difference between the two months. In 2017 and 2018, the PAN concentration decreased due to the effect of vertical mixing during the daytime because of the strong vertical turbulence. Chemical reactions mainly contributed to an increase in PAN concentration, which reflects the relatively intensive chemical production rates during the daytime. The results demonstrated that the horizontal

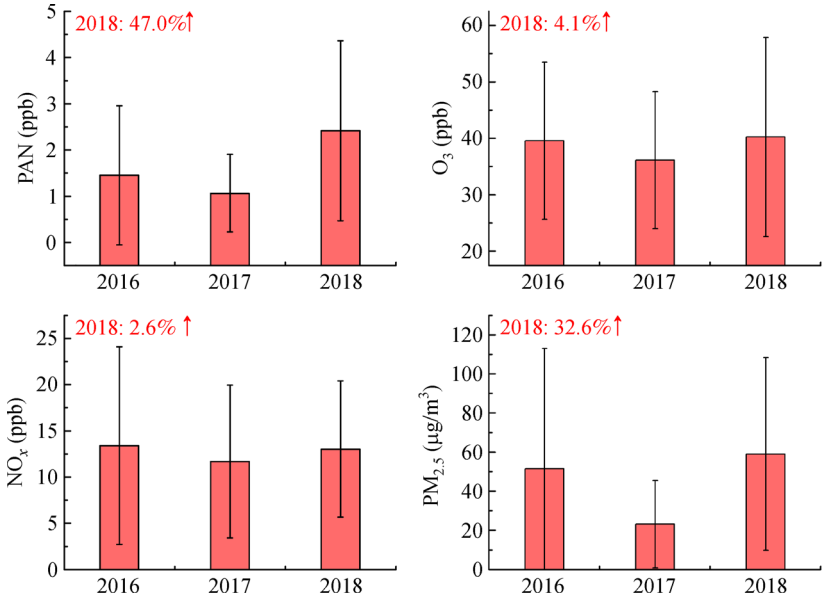

Fig. 7 Monthly mean concentrations of PAN (ppb), O_3 (ppb), NO_x (ppb) and $PM_{2.5}$ (μg/m^3) from March 2016 to 2018. The whiskers represent the standard deviation. The red values in the upper left corners denote the changes rates in 2018 compared with mean values from 2016 to 2018.

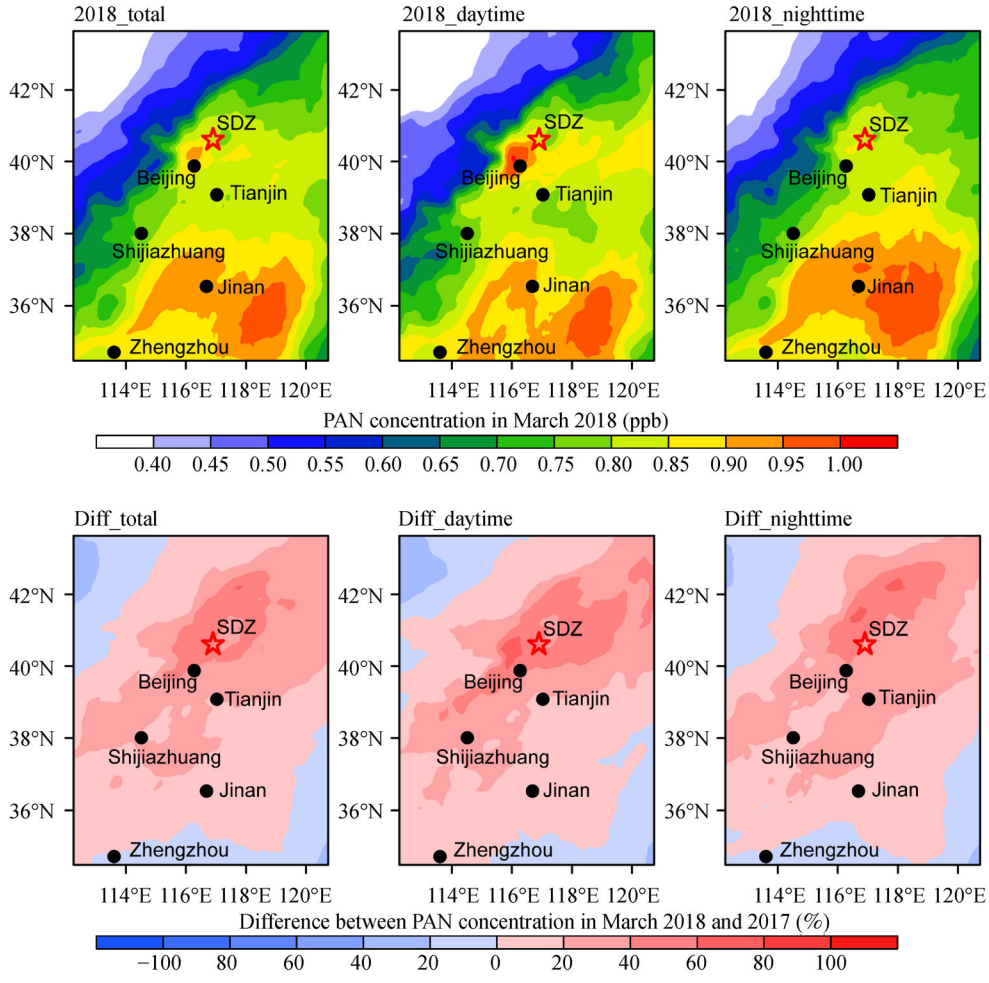

Fig. 8 Simulated surface-layer PAN concentrations (ppb) in March 2018 (top) and the differences between the PAN concentrations (%) in March of 2018 and 2017. The three columns represent the PAN concentrations throughout the whole day, in the daytime and in the nighttime, respectively. The red stars represent the position of the SDZ site.

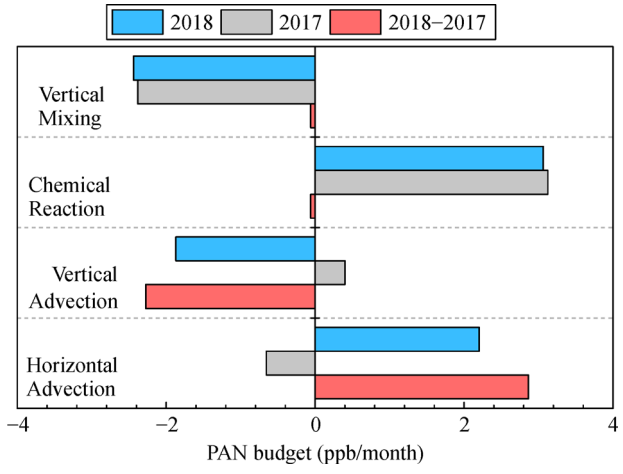

Fig. 9 Simulated monthly PAN changes induced by each physical/chemical process averaged over the NCP region in March of 2017 and 2018 during the daytime (8:00–20:00) as well as the difference between the two months.

advection in March 2018 resulted in a notable increase in PAN concentration, while that in 2017 had the opposite effect. As shown in Fig. 10, the NCP region was dominated by a high pressure and north-westerly wind in 2017. However, in March 2018, the region was in front of a low-pressure system, and the prevailing wind was south-westerly. Therefore, in March 2018, PAN and its precursors were more likely to accumulate, resulting in a positive contribution of horizontal advection. Considering that the PAN lifetime was approximately several days in spring, this effect contributed the most to the difference between the PAN concentrations in these two months, which might be the main cause of the simulated increase in 2018. This effect could imply that, except for aerosol pollution, the extreme events with high concentrations of PAN in spring should also cause much concern during stable conditions.

Although the model captured the increasing trend of the PAN concentration at the SDZ site, the simulated increase

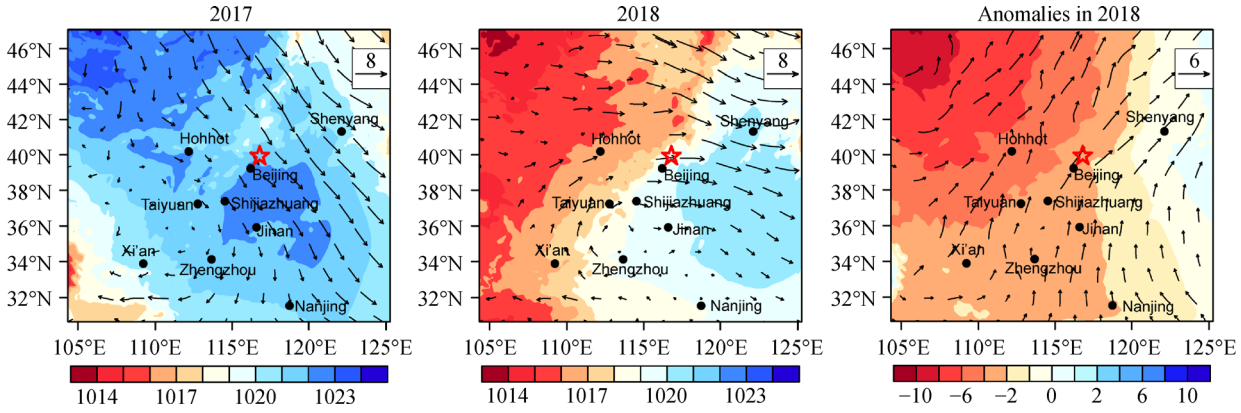

Fig. 10 Simulated monthly mean winds at 850 hPa and sea-level pressure (hPa) in March of 2017 and 2018 as well as the difference (2018–2017) between the simulated winds. The red stars represent the position of the SDZ site.

rate (47%) was still lower compared with the observed increase rate (118%). We inferred that the model failed to capture the high PAN concentration in very polluted episodes due to the uncertainties in VOC emissions (Qiu et al., 2019a) and PAN formation through reactions with aromatics (Fischer et al., 2014). In this study, the underestimation of simulated PAN concentrations reached to 31% and 49% in March 2017 and March 2018, respectively. Thus, in the future, greater efforts are needed to include any chemical mechanisms that may be missing and to evaluate the uncertainties in VOC emissions in the WRF-Chem model.

4 Conclusions

In this study, we monitored the PAN, O_3 and NO_x concentrations at the SDZ regional background site from August 2015 to February 2019. Based on the observation results, we analyzed the diurnal and seasonal variations in PAN and the cause of the high PAN concentrations in spring 2018. The main conclusions are as follows:

1) The continuous measurement results from August 2015 to February 2019 at the SDZ site showed that the monthly mean PAN concentration varied from 0.33–2.41 ppb, with an average value of 0.94 ppb. The maximum and minimum mean PAN concentrations occurred in January 2016 and March 2018, respectively. The PAN concentration exhibited notable seasonal variations, with high values in spring and low values in winter. O_3 usually reached its maximum values from May to August annually at the background site, which was slightly later than what was observed for PAN. Regarding the diurnal variations, the PAN concentration at the SDZ site generally reached its maximum values from 16:00–18:00, which was slightly later than what was previously reported at urban sites. Specifically, the diurnal variation was much weaker in winter than those in the other seasons, implying a low production and a relatively longer lifetime in the winter.

2) Based on the observation results at the SDZ site, the maximum seasonal mean concentrations occurred in spring and were 51.0% higher than the values averaged over the whole observation period. As the emission rates of PAN precursors were low in spring, we attributed the high PAN concentrations in spring to the differences in meteorology and background concentration. After analyzing the corresponding meteorological data, we found that the more intense UV radiation, the relatively longer lifetime in spring, the much shorter lifetime and higher precipitation in summer contributed to the higher PAN concentration in spring compared to that in summer. In addition, the high background PAN concentrations, which accounted for approximately 28% of the mean PAN concentrations in spring, was 55.5% higher than the average background concentration. This effect might also have contributed to the increased PAN concentration in spring.

3) The observation results revealed that the maximum monthly PAN concentration at the SDZ site occurred in March 2018 with a mean value of 2.4 ppb. To examine the cause of the high PAN concentration at that time, we performed WRF-Chem simulations in March of 2017 and 2018 at the same emission rate. The model results demonstrated that the simulated PAN concentrations in March 2018 were notably higher than those in 2017 across most of the NCP region. The increase rate even ranged from 40%–60% in Beijing and the northern part of the NCP region. The simulation results further showed that the anomalously low pressure and the southwesterly winds in northern China might be the main causes of the increase in Beijing and its surrounding area in 2018.

In this study, we examined the PAN concentration at a background site near Beijing and its diurnal, seasonal and interannual variations based on continuous measurements from August 2015 to February 2019. Using multiple observations and model simulation results, we attributed the cause of the seasonal and interannual PAN concentration variations to the changes in meteorology and back-

ground concentration. Although the WRF-Chem model captured the basic features of PAN in northern China, it still has difficulty in simulating heavily polluted episodes. In the future, we need to improve the model performance in simulating the PAN concentration over China to better understand the photochemical pollution in this region.

Acknowledgements The authors would like to thank the staff of the Shangdianzi station for their excellent work. This research is supported by the Beijing Natural Science Foundation (Grant No. 8194078), National Key R&D Program of China (Grant No. 2016YFC0201902), National Natural Science Foundation of China (Grant No. 91744206). All of the observational data and modeling results have been archived by the corresponding author, Prof. Zhiqiang Ma (zqma@ium.cn) and are available upon request.

References

Beine H, Krognes T (2000). The seasonal cycle of peroxyacetyl nitrate (PAN) in the European Arctic. Atmospheric Environment, 34(6): 933–940

Beine H J, Jaffe D A, Blake D R, Atlas E, Harris J (1996). Measurements of PAN, alkyl nitrates, ozone and hydrocarbons during spring in interior Alaska. Journal of Geophysical Research, 101(D7): 12613–12619

Brice K A, Penkett S A, Atkins D H F, Sandalls F J, Bamber D J, Tuck A F, Vaughan G (1984). Atmospheric measurements of peroxyacetyl nitrate (PAN) in rural, south-east England: Seasonal variations winter photochemistry and long-range transport. Atmospheric Environment, 18(12): 2691–2702

Bukowiecki N, Dommen J, Prevot A S H, Richter R, Weingartner E, Baltensperger U (2002). A mobile pollutant measurement laboratory—Measuring gas phase andaerosol ambient concentrations with high spatial and temporal resolution. Atmospheric Environment, 36 (36-37): 5569–5579

Chen L, Zhu J, Liao H, Gao Y, Qiu Y, Zhang M, Liu Z, Li N, Wang Y (2019). Assessing the formation and evolution mechanisms of severe haze pollution in the Beijing–Tianjin–Hebei region using process analysis. Atmospheric Chemistry and Physics, 19(16): 10845–10864

Chou M D, Suarez M J, Ho C H, Yan M M H, Lee K T (1998). Parameterizations for cloud overlapping and shortwave single-scattering properties for use in general circulation and cloud ensemble models. Journal of Climate, 11(2): 202–214

Fischer E V, Jacob D J, Yantosca R M, Sulprizio M P, Millet D B, Mao J, Paulot F, Singh H B, Roiger A, Ries L, Talbot R W, Dzepina K, Pandey Deolal S (2014). Atmospheric peroxyacetyl nitrate (PAN): A global budget and source attribution. Atmospheric Chemistry and Physics, 14(5): 2679–2698

Fischer E V, Jaffe D A, Reidmiller D R, Jaeglé L (2010). Meteorological controls on observed peroxyacetyl nitrate at Mount Bachelor during the spring of 2008. Journal of Geophysical Research, 115(D3): D03302

Gaffney J S, Marley N A, Prestbo E W (1993). Measurements of peroxyacetyl nitrate at a remote site in the southwestern United States: Tropospheric implications. Environmental Science & Technology, 27(9): 1905–1910

Gao J, Zhu B, Xiao H, Kang H, Pan C, Wang D, Wang H (2018). Effects of black carbon and boundary layer interaction on surface ozone in Nanjing, China. Atmospheric Chemistry and Physics, 18(10): 7081–7094

Gao T, Han L, Wang B, Yang G, Xu Z, Zeng L, Zhang J (2014). Peroxyacetyl nitrate observed in Beijing in August from 2005 to 2009. Journal of Environmental Sciences (China), 26(10): 2007–2017

Guenther A, Karl T, Harley P, Wiedinmyer C, Palmer P I, Geron C (2006). Estimates of global terrestrial isoprene emissions using MEGAN (Model of Emissions of Gases and Aerosols from Nature). Atmospheric Chemistry and Physics, 6(11): 3181–3210

Heuss J M, Glasson W A (1968). Hydrocarbon reactivity and eye irritation. Environmental Science & Technology, 2(12): 1109–1116

Hong S Y, Jade Lim J O (2006). The WRF single-Moment 6-class microphysics Scheme. Journal of the Korean Meteorological Society, 42: 129–151

Hong S Y, Noh Y, Dudhia J (2006). A new vertical diffusion package with an explicit treatment of entrainment processes. Monthly Weather Review, 134(9): 2318–2341

Jiang F, Zhou P, Liu Q, Wang T, Zhuang B, Wang X (2012). Modeling tropospheric ozone formation over East China in springtime. Journal of Atmospheric Chemistry, 69(4): 303–319

Lee J B, Yoon J S, Jung K, Eom S W, Chae Y Z, Cho S J, Kim S D, Sohn J R, Kim K H (2013). Peroxyacetyl nitrate (PAN) in the urban atmosphere. Chemosphere, 93(9): 1796–1803

Li K, Jacob D J, Liao H, Shen L, Zhang Q, Bates K H (2019). Anthropogenic drivers of 2013–2017 trends in summer surface ozone in China. Proceedings of the National Academy of Sciences of the United States of America, 116(2): 422–427

Li L, Wu F K, Meng X Y (2013). Seasonal and diurnal variation of isoprene in the atmosphere of Beijing. Environmental Monitoring in China, 29(2): 120–124

Li M, Zhang Q, Kurokawa J I, Woo J H, He K, Lu Z, Ohara T, Song Y, Streets D G, Carmichael G R, Cheng Y, Hong C, Huo H, Jiang X, Kang S, Liu F, Su H, Zheng B (2017). MIX: A mosaic Asian anthropogenic emission inventory under the international collaboration framework of the MICS-Asia and HTAP. Atmospheric Chemistry and Physics, 17(2): 935–963

Liu L, Wang X, Chen J, Xue L, Wang W, Wen L, Li D, Chen T (2018). Understanding unusually high levels of peroxyacetyl nitrate (PAN) in winter of urban Jinan, China. Journal of Environmental Sciences (China), 71(9): 249–263

Liu Z, Wang Y, Gu D, Zhao C, Huey L G, Stickel R, Liao J, Shao M, Zhu T, Zeng L, Liu S C, Chang C C, Amoroso A, Costabile F (2010). Evidence of reactive aromatics as a major source of peroxyacetyl nitrate over China. Environmental Science & Technology, 44(18): 7017–7022

Ma Z, Xu J, Quan W, Zhang Z, Lin W, Xu X (2016). Significant increase of surface ozone at a rural site, north of eastern China. Atmospheric Chemistry and Physics, 16(6): 3969–3977

McFadyen G G, Cape J N (2005). Peroxyacetyl nitrate in eastern Scotland. Science of the Total Environment, 337(1–3): 213–222

Mlawer E J, Taubman S J, Brown P D, Iacono M J, Clough S A (1997). Radiative transfer for inhomogeneous atmospheres: RRTM, a validated correlated-k model for the longwave. Journal of Geophy-

sical Research, D, Atmospheres, 102(D14): 16663–16682

Monson R K, Jaeger C H, Adams W W III, Driggers E M, Silver G M, Fall R (1992). Relationships among isoprene emission rate, photosynthesis, and isoprene synthase activity as influenced by temperature. Plant Physiology, 98(3): 1175–1180

Moxim W J, Levy H II, Kasibhatla P S (1996). Simulated global tropospheric PAN: Its transport and impact on NO_x. Journal of Geophysical Research, 101(D7): 12621–12638

Penkett S A, Brice K A (1986). The spring maximum in photo-oxidants in the Northern Hemisphere troposphere. Nature, 319(6055): 655–657

Pandey Deolal S, Henne S, Ries L, Gilge S, Weers U, Steinbacher M, Staehelin J, Peter T (2014). Analysis of elevated springtime levels of Peroxyacetyl nitrate (PAN) at the high Alpine research sites Jungfraujoch and Zugspitze. Atmospheric Chemistry and Physics, 14(22): 12553–12571

Qiu Y, Lin W, Li K, Chen L, Yao Q, Tang Y, Ma Z (2019b). Vertical characteristics of peroxyacetyl nitrate (PAN) from a 250-m tower in northern China during September 2018. Atmospheric Environment, 213: 55–63

Qiu Y, Ma Z, Li K (2019a). A modeling study of the peroxyacetyl nitrate (PAN) during a wintertime haze event in Beijing, China. Science of the Total Environment, 650: 1944–1953

Rappenglück B, Kourtidis K, Fabian P (1993). Measurements of ozone and peroxyacetyl nitrate (PAN) in Munich. Atmospheric Environment, 27(3): 293–305

Schmitt R, Volz-Thomas A (1997). Climatology of ozone, PAN, CO, and NMHC in the free troposphere over the southern North Atlantic. Journal of Atmospheric Chemistry, 28(1/3): 245–262

Seinfeld J H, Pandis S N (2006). Atmospheric chemistry and physics: From air pollution to climate change. 2nd, ed. Hoboken: John Wiley & Sons, Inc., 231–233

Singh H B, Hanst P L (1981). Peroxyacetyl nitrate (PAN) in the unpolluted atmosphere: An important reservoir for nitrogen oxides. Geophysical Research Letters, 8(8): 941–944

Singh H B, Salas L J (1989). Measurements of peroxyacetyl nitrate (PAN) and peroxypropionyl nitrate (PPN) at selected urban, rural and remote sites. Atmospheric Environment, 23(1): 231–238

Singh H B, Salas L J, Ridley B A, Shetter J D, Donahue N M, Fehsenfeld F C, Fahey D W, Parrish D D, Williams E J, Liu S C, Hubler G, Murphy P C (1985). Relationship between peroxyacetyl nitrate and nitrogen oxides in the clean troposphere. Nature, 318(6044): 347–349

Singh H B, Salas L J, Viezee W (1986). Global distribution of peroxyacetyl nitrate. Nature, 321(6070): 588–591

Sun E J, Huang M H (1995). Detection of peroxyacetyl nitrate at phytotoxic level and its effects on vegetation in Taiwan. Atmospheric Environment, 29(21): 2899–2904

Talukdar R K, Burkholder J B, Schmoltner A M, Roberts J M, Wilson R R, Ravishankara A R (1995). Investigation of the loss processes for peroxyacetyl nitrate in the atmosphere: UV photolysis and reaction with OH. Journal of Geophysical Research, D, Atmospheres, 100 (D7): 14163–14173

Tanner R L, Miguel A H, de Andrade J B, Gaffney J S, Streit G E (1988). Atmospheric chemistry of aldehydes: enhanced peroxyacetyl nitrate formation from ethanol-fueled vehicular emissions. Environmental Science & Technology, 22(9): 1026–1034

Taylor O C (1969). Importance of peroxyacetyl nitrate (PAN) as a phytotoxic air pollutant. Journal of the Air Pollution Control Association, 19(5): 347–351

Temple P J, Taylor O C (1983). World-wide ambient measurements of peroxyacetyl nitrate (PAN) and implications for plant injury. Atmospheric Environment, 17(8): 1583–1587

Wang B, Shao M, Roberts J M, Yang G, Yang F, Hu M, Zeng L, Zhang Y, Zhang J (2010). Ground-based on-line measurements of peroxyacetyl nitrate (PAN) and peroxypropionyl nitrate (PPN) in the Pearl River Delta, China. International Journal of Environmental Analytical Chemistry, 90(7): 548–559

Wang Y S, Yao L, Wang L L, Liu Z R, Ji D S, Tang G Q, Zhang J K, Sun Y, Hu B, Xin J Y (2014). Mechanism for the formation of the January 2013 heavy haze pollution episode over central and eastern China. Science China. Earth Sciences, 57(1): 14–25

Xue L, Wang T, Wang X, Blake D R, Gao J, Nie W, Gao R, Gao X, Xu Z, Ding A, Huang Y, Lee S, Chen Y, Wang S, Chai F, Zhang Q, Wang W (2014). On the use of an explicit chemical mechanism to dissect peroxyacetyl nitrate formation. Environmental Pollution, 195: 39–47

Yin Z, Wang H, Ma X (2019). Possible relationship between the Chukchi sea ice in the early winter and the February haze pollution in the North China Plain. Journal of Climate, 32(16): 5179–5190

Zaveri R A, Easter R C, Fast J D, Peters L K (2008). Model for simulating aerosol interactions and chemistry (MOSAIC). Journal of Geophysical Research-Atmosphere, 113:D13204

Zaveri R A, and Peters L K (1999). A new lumped structure photochemical mechanism for large-scale applications. Journal of Geophysical Research, 104(D23): 30387–30415

Zhang B, Zhao B, Zuo P, Huang Z, Zhang J (2017). Ambient peroxyacyl nitrate concentration and regional transportation in Beijing. Atmospheric Environment, 166: 543–550

Zhang G, Mu Y, Zhou L, Zhang C, Zhang Y, Liu J, Fang S, Yao B (2015). Summertime distributions of peroxyacetyl nitrate (PAN) and peroxypropionyl nitrate (PPN) in Beijing: Understanding the sources and major sink of PAN. Atmospheric Environment, 103: 289–296

Zhang H, Xu X, Lin W, Wang Y (2014). Wintertime peroxyacetyl nitrate (PAN) in the megacity Beijing: Role of photochemical and meteorological processes. Journal of Environmental Sciences (China), 26(1): 83–96

Zhang J M, Wang T, Ding A J, Zhou X H, Xue L K, Poon C N, Wu W S, Gao J, Zuo H C, Chen J M, Zhang X C, Fan S J (2009). Continuous measurement of peroxyacetyl nitrate (PAN) in suburban and remote areas of western China. Atmospheric Environment, 43(2): 228–237

Zhu H, Gao T, Zhang J (2018). Wintertime characteristic of peroxyacetyl nitrate in the Chengyu district of southwestern China. Environmental Science and Pollution Research International, 25(23): 23143–23156